Published in final edited form as:
J Comp Neurol. 2009 May 10; 514(2): 161–173. doi:10.1002/cne.22004.

Birth of ophthalmic trigeminal neurons initiates early in the placodal ectoderm

Kathryn L. McCabe[1,*], **John W. Sechrist**[1,*], and **Marianne Bronner-Fraser**[1]

[1]Division of Biology 139-74, California Institute of Technology, Pasadena, CA, 91125, Office (626) 395-3355, Fax (626) 449-8599

Abstract

The largest of the cranial ganglia, the trigeminal ganglion relays cutaneous sensations of the head to the central nervous system. Its sensory neurons have a dual origin from both ectodermal placodes and neural crest. Here, we show that birth of neurons derived from the chick ophthalmic trigeminal placode begins prior to their ingression (HH11), as early as HH8, and considerably earlier than previously suspected (HH16). Furthermore, cells exiting the cell cycle shortly thereafter express the ophthalmic trigeminal placode marker Pax3 (HH9). At HH11, these post-mitotic Pax3+ placode cells begin to express the pan neuronal marker, neurofilament, while still in the ectoderm. Analysis of the ectodermal origin and distribution of these early post-mitotic neurons reveals that the ophthalmic placode extends further rostrally than anticipated, contributing to neurons that reside in and make a significant contribution to the ophthalmic trigeminal nerve. These data redefine the timing and extent of neuron formation from the ophthalmic trigeminal placode.

Keywords

trigeminal placode; BrdU; thymidine; birthdate; neuron

Introduction

The trigeminal ganglion, providing cutaneous sensory innervation for much of the face, is comprised of two distinct lobes that differ in morphology and projection patterns. The ophthalmic lobe innervates the forehead, eyes, and nose, whereas the maxillomandibular innervates the jaw, teeth, and tongue. Although the later steps of ganglion formation and guidance of trigeminal axons to their targets have been studied extensively (rev. Baker and Bronner-Fraser, 2001), less is known about early events governing neuronal differentiation, distribution and aggregation. The trigeminal ganglion owes its embryonic origin to two different cell populations—trigeminal placode and neural crest. Whilst placode cells uniquely form sensory neurons, neural crest contributes to both sensory neurons and glia. In birds, these two cell populations intermix but are morphologically distinguishable for the first two weeks of development by size and location (D'Amico-Martel and Noden, 1980).

When and how does the trigeminal ganglion begin to form? Previous studies have shown that secreted factors from the dorsal neural tube induce the ophthalmic trigeminal (opV) placode (Stark et al., 1997; Baker et al., 1999) in a manner that requires Platelet Derived

Author of Correspondence mbronner@caltech.edu.
*Both authors contributed equally to this paper.
Associate Editor: John L. R. Rubenstein

Growth Factor signaling (McCabe and Bronner-Fraser, 2008). In chick, this induction process begins around HH8 (Stark et al., 1997; Baker et al., 1999) and ectoderm becomes specified to express Pax3 protein, a molecular marker for opV placode, around HH9 (8ss) (Baker et al., 1999). Pax3 mRNA is expressed in the presumptive forebrain/midbrain neural folds as early as HH8 in embryos with four somite pairs (Stark et al., 1997). Individual opV placode cells express Delta-1, Brn3a, and the tetraspanin CD151 around HH10 (Begbie et al., 2002; McCabe et al., 2004). The first opV placode cells ingress as spurs or individual cells at HH11 (D'Amico-Martel and Noden, 1983) and express the neuronal marker, β-tubulin by HH13 in the placodal ectoderm and forming opV ganglion (Moody et al., 1989). DiI labeling of the surface ectoderm at HH11 has shown that, in addition to their well known origin from midbrain level ectoderm (D'Amico-Martel and Noden, 1980; Xu et al., 2008) placodal opV neurons also arise from caudal forebrain (Lee et al., 2003). By HH14–16, ingressing opV placode cells are numerous and conspicuous, apparently completing ingression by HH21 (D'Amico-Martel and Noden, 1983).

The early appearance of neuronal markers in the opV placode even prior to ingression raises the intriguing possibility that some placode cells may be post-mitotic while still in the ectoderm. However, surprisingly little is known about their earliest time of cell cycle exit. To help interpret emerging molecular information on trigeminal placode development (McCabe et al., 2004, 2007), it is important to determine the link between cell cycle exit and processes of induction and specification. D'Amico-Martel and Noden (1980) reported that trigeminal placode cells contributing to the maxillomandibular (mmV) lobe first exit the cell cycle at HH16 and continue becoming post-mitotic through HH30, when only satellite cells are labeled. Although almost all data presented was for the mmV lobe, their summary diagram suggested that birth of opV placode cells may be similar. More recent work (Begbie et al., 2002) reports that ingressing opV placode cells at HH13 lack phosphohistoneH3, a marker for dividing cells (Hendzel et al., 1997), suggesting that they may be born at earlier stages than previously thought.

To rigorously evaluate the birthdate of opV placode cells, we combine labeling with ^{3}H-Thymidine (^{3}H-Thy) and bromodeoxyuridine (BrdU), with molecular markers, to show that cell cycle exit and differentiation initiates within the early placode prior to ingression and that the opV placode extends more rostrally than previously thought. These data form a critical framework for understanding molecular aspects of ophthalmic trigeminal ganglion formation as well as interpreting events leading to malformations of the ganglion or misroutings of the opV nerve in the adult.

Methods and Materials

^{3}H-Thymidine and BrdU labeling

Embryos were staged according to Hamburger and Hamiliton (1951) for ^{3}H-Thymidine (New England Nuclear; 6.7 Ci/mmol) and BrdU (Sigma) labeling. Embryos received two, 50λ injections of 10–40 μCi of ^{3}H-Thymidine in PBS (pH 7.4) separated by 3 hours, to provide complete coverage for all dividing cells, and incubated until desired stage at 37°C (n= 2 for HH6–7 (headfold- 2 somite stage (ss)), n=1 for HH8 (3–5ss), n=1 for HH10 (9–11ss), n=2 for HH11 (12–14ss), n=1 for HH12 (15–17ss), n=2 for HH14 (21–23ss)). Fixation and autoradiography was performed as previously described (Sechrist and Bronner-Fraser, 1991; Sechrist and Marcelle, 1996).

All ^{3}H-Thymidine sections were counterstained with Toluidine blue to allow identification of cytoplasm from nuclei and nucleoli. Cytoplasmic material stains a darker shade of purple than the nucleus. The circular nuclei are seen as a lighter shade of purple with intensely purple spots that mark the nucleoli within the nucleus. Note that sections are 1 μm thin, and

therefore do not always contain a nucleus. When this occurs, serial sections are consulted to determine the labeling of a given nucleus with silver grains. Determination of level of labeling was done on a case by case basis as changes in exposure time of autoradiography changes the apparent density of silver grains. Heavily labeled cells were actively dividing at the time of application. Some cells had significantly lighter label and may have been at the end of their final DNA synthesis phase and the second application of ^{3}H-Thymidine three hours later during what would have been another S phase was not incorporated. These cells were counted as dividing. Cells that contained no grains above background silver grains were considered to have exited the cell cycle.

In order to co-label cells for cell division and molecular markers, the thymidine analog, bromodeoxyuridine (BrdU) (40–75 λ of 10–100 μM BrdU) was applied directly to the embryos, twice in a 2–3 hour interval to ensure that all cells undergoing DNA synthesis would be labeled, and incubated until desired stage at 37°C (n=5 for HH6–7, n=8 for HH8, n=8 for HH9 (6–8ss), n=9 for HH10). Cumulative labeling experiments described above mark all dividing cells at the time of application. On the other hand, the pulse labeling experiments described below give a quick snap shot of those cells in S phase for 30 minutes. For pulse labeling experiments embryos were exposed to BrdU for 30 minutes, and then immediately fixed in 4% paraformaldehyde at room temperature for 4 hours (n=1 for HH9, n=2 for HH10, n=5 for HH11, n=5 for HH12, n=8 for HH16 (28–30ss)). Embryos were cryoprotected and cryosectioned at 8 μm as previously described (Sechrist et al., 1995) with the exception of the Pax3 images in Figure 2 which were cut at 10 μm.

Digital Photography

All DIC photographs were taken using the Zeiss Axioskop2 using the Axiocam HRC digital camera. All fluorescent images were taken using the Zeiss Axioskop2 Plus using the Axiocam mRM digital camera with the following exceptions which were photographed on 35mm slide film on the Olympus Vanox microscope: Figure 2C and Figure 3I–K. 35mm slides were scanned into digital format using the Epson Perfection 3200 photo or Agfa Snap Scan 310. All figures were adjusted for optimal brightness and contrast in Photoshop 7.0. Images were subsequently imported into Illustrator 10 to apply labels. Some color change was noticed during the importation and was subsequently adjusted back to the levels original to the Photoshop images.

Immunostaining

Immunostaining was performed as described (Sechrist et al., 1995) with the exception of the boric acid treatment for BrdU staining (P. Strobl, personal communication). Sections were subjected to 2N HCl in PBS for 30 minutes at room temperature, 0.1 M Boric Acid pH 6 in PBS for 20 minutes, and rinsed in PBS three times prior to immunostaining. Primary antibodies were used at the following concentrations: BrdU (Sigma, 1:1000), Phosphohistone H3 (Upstate biotechnology, 1:250), HuC/D (Invitrogen, 1:200), Neurofilament 145 kDa (Chemicon, 1:500), Pax3 (Developmental Hybridoma Bank, 1: 10). Secondary antibodies conjugated with Alexa 488 and 568 (Molecular Probes) were used at 1:1000 (Goat anti-rabbit and Goat anti-mouse IgG1, IgG2a, IgG2b). For detection of nuclei, DAPI (Sigma) at 2 μg/ml in PBS for 10 minutes at room temperature.

The identification, specificity, and controls for each primary antibody utilized are as follows: Anti-BrdU is a mouse antiserum (Sigma #B-2531, Lot 074H4814) prepared against BromodeoxyUridine conjugated to KLH. The specificity of the antiserum was tested by Elisa, flow cytometry, and no BrdU controls (Gratzner, 1982; Meyer et al., 1989). Anti-PhosphoHistone H3 is a rabbit polyclonal (Upstate Biotechnology # 06-570, Lot DAM1416518) prepared against peptide ARKpSTGGKAPRKQLC corresponding to amino

acids 7–20 of human histone H3. The antibody stains a single band of 17kDa molecular weight on Western blot (manufacturer's technical information). Controls were done by Western blot on acid extracts of colcemid treated and untreated human HeLa cell lines. Anti-HuC/D is a mouse monoclonal (Invitrogen #A21271, Lot 43471A) prepared against Human peptide QAQRFRLDNLN-C-Keyhole Limpet Hemocyanin conjugate. The antibody stains three Hu bands, HuDpro, HuD, and HuC in human cortical neuronal extracts. The HuC/D does not bind to the HuDmex peptide that is missing the immunized domain or unrelated proteins (Marusich et al., 1993). Anti-Neurofilament is a rabbit polyclonal (Chemicon #AB1987, Lot 0512018314) prepared against the recombinant fusion protein containing the C-terminal 168 amino acids of rat NF-M. The antibody stains a single band at 145kDa molecular weight on chicken brain extract on Western blot (Harris et al., 1991). This antibody provides the same staining in the developing chick retina as the antibody, RMO270, a mouse monoclonal against NFM (McCabe et al., 1999; McCabe et al., 2005). Anti-Pax3 is a mouse monoclonal (Developmental Hybridoma Bank #Pax3) prepared against the recombinant fusion protein containing C-terminal region (amino acid #298-481) of Quail Pax3. The antibody stains a single band at approximately 60 kDa on E3 chicken neural tube and notochord extract on Western blot (Venters et al., 2004). The expression of Pax3 protein is similar to previously reported mRNA (Stark et al., 1997; Baker et al., 1999).

DiI labeling

In order to label the surface ectoderm without labeling the neural tube or neural crest, whole embryos were labeled with 0.5% DiI (Molecular Probes) after cranial neural tube closure (HH10) as previously described (Sechrist et al., 1995; Stark et al., 1997).

Results

Cumulative labeling of embryos with ^{3}H-Thy or the thymidine analog, BrdU, was performed at stages ranging from HH7–14 to determine the time and location that the first opV placode cells cease DNA synthesis using established criteria (Sidman, 1970). To achieve cumulative labeling, two doses of ^{3}H-Thy or BrdU were applied 3hrs apart to ensure uptake by all dividing cells when the cell cycle time is approximately 8hrs (Langman et al., 1966; Sechrist and Bronner-Fraser, 1991). Embryos were collected at selected intervals between 10 and 32 hours of total incubation times. Initial experiments were performed with ^{3}H-Thy, as it has several advantages. First, it is readily incorporated at non-toxic concentrations, allowing for embryo collection after longer incubation periods. Second, ^{3}H-Thy treated embryos can be embedded in plastic and sectioned at 0.5–1μm allowing for high resolution analysis and exact identification of ^{3}H-Thy incorporation by nuclei. Third, the amount of incorporation can be analyzed by grouping the cells into 3 classes: no label, light label or heavy label. On the other hand, BrdU labeling offers the possibility of performing double antibody labeling. BrdU labeling also provides relatively quick verification of data obtained from ^{3}H-Thy labeling.

All ^{3}H-Thy sections were counterstained with Toluidine Blue to allow for identification of cytoplasm, nuclei, and nucleoli. Cytoplasm is characterized by its darker purple stain, while nuclei are a lighter purple and circular in shape within the cytoplasm. In addition, nucleoli show up as intensely dark purple spots within the nucleus. Since the sections are only 1 μm thick, there are instances where the nucleus will appear on an adjacent section. To verify the lack of label, serial sections were examined to clearly identify cells that contain a nucleus and whether this nucleus is labeled with silver grains. Notably, many nuclei are heavily labeled and are easily identifiable as actively dividing at the time of ^{3}H-Thy application. However, there are two additional classes of cells, those that are lightly labeled and those that are unlabeled. Lightly labeled cells were identified as having significantly fewer grains of silver above background than heavily labeled cells. These cells are likely lightly labeled

due to only incorporating ^{3}H-Thy during the first application and exiting the cell cycle before the second application three hours later. None the less, these cells were identified as actively dividing at the time of application. Only cells with no grains above background levels were classified as post-mitotic.

Some opV placode cells become post-mitotic in the ectoderm at HH8

We tested when the first opV placode cells exit the cell cycle. Exposure of embryos to ^{3}H-Thy or BrdU at HH7 resulted in labeling of all cells, indicating that presumptive opV placode cells have yet to exit the cell cycle; e.g., an embryo treated with ^{3}H-Thy at HH7 and allowed to develop to HH13 has ophthalmic placode cells in the process of delaminating from the ectoderm at midbrain and rostral hindbrain levels (Figure1A–C); their parent cells were still actively dividing as indicated by silver grains over the nuclei. Similar data were obtained using BrdU labeling (Figure4A–C). This suggests that few if any opV precursor cells have ceased dividing at HH7.

Interestingly, application of either ^{3}H-Thy or BrdU at HH8 revealed a few scattered cells in the presumptive opV placode that have exited the cell cycle. From the middle forebrain to rostral hindbrain, ≥45 cells within the dorsolateral ectoderm and adjacent mesenchyme lacked ^{3}H-Thy incorporation (summarized in Figure1D). Figure1E–H show delaminating placode cells at the forebrain, rostral and middle midbrain levels that have failed to incorporate ^{3}H-Thy (arrow). However, most opV placode cells have not yet begun to exit the cell cycle at rostral hindbrain levels (arrowhead; Figure1I). In contrast, labeling at HH10 yields increased numbers of post-mitotic cells (≥85) including some that have ingressed at more caudal levels (Figure 3A,B). These results suggest that there is a rostrocaudal gradient of cell cycle exit with more rostral opV cells being born first (Figure 1E–I), and cells at the level of the caudal midbrain/rostral hindbrain generated somewhat later (Figure1H–I, Figure3C–G).

Distribution of post-mitotic cells suggests a rostral extension of the opV placode

To assess the distribution of opV precursors throughout the ectoderm, we systematically analyzed all available cranial sections through an embryo treated with ^{3}H-Thy at HH8 and collected at HH12. The region of interest included 80 slides with approximately 15 sections/slide at 1μm thick. The position of unlabeled cells within the ectoderm (red circle) or adjacent mesenchyme (green triangle) were marked according to their rostrocaudal and mediolateral locations relative to forebrain, midbrain, and rostral hindbrain (Figure1D). Ingressing ectodermal cells and cells beginning to condense to form the trigeminal ganglion and nerve were classified as mesenchymal. These earliest post-mitotic cells extended from mid-forebrain to rostral-hindbrain levels. From medial to lateral, the unlabeled cells were found above and lateral to the neural tube (Figure1E) within the Pax3 protein expression domain (Figure2G–I). Figure1E shows at least three clustered cells that are ^{3}H-Thy negative, two of which have ingressed from the ectoderm at the caudal forebrain/rostral foregut level. Additional individual cells at the rostral midbrain level can be seen exiting the ectoderm (Figure 1F–G). Slightly later (HH10 label, collected at HH15), there are two ^{3}H-Thy negative cells in the mesenchyme at the level of the forebrain corresponding to the presumptive path on which the ophthalmic nerve will project (Figure 2A–B). Initially, their position is dorsal to the eye but shifts medially at later stages. To confirm that these post-mitotic cells are neurons, we treated an embryo at HH9 (collected at HH15) with BrdU. Similar BrdU- cells were noted between the eye and forebrain expressing neurofilament (NFM); note NFM nerve fibers (green) surrounding the DAPI (blue) stained nuclei lacking BrdU (red; Figure2D–F). Using the trigeminal placode marker Pax3 at HH9–11, we find Pax3+ placodal ectodermal cells at the level of the forebrain (Figure 2G–I), further

supporting the idea that the trigeminal placode extends to the caudal forebrain level ectoderm.

To verify the site of origin of these cells, we labeled the ectoderm at HH11 with DiI, after neural tube closure. This allows complete labeling of ectoderm but not the neural tube or neural crest. Accordingly, any DiI positive cells within the mesenchyme are ectodermally derived and therefore of placodal origin. Figure2C shows DiI-labeled ectoderm at HH11, processed at HH14. Several cells have migrated in a stream, delaminating at the forebrain level (Figure2C), and localizing in the vicinity of the future ophthalmic nerve. Thus, DiI-labeled placode cells from rostral ectoderm contribute neuronal cell bodies to the opV nerve. Co-staining with neurofilament antibodies (data not shown) verifies that these cells selectively contribute to neurons along the ophthalmic nerve.

Analysis of serial sections through embryos treated at HH10 and HH14 confirms that post-mitotic neuronal cell bodies lie along the opV nerve. Some of these scattered cells at eye level or just caudal to the eye are found as individuals or in strands of two to four cells (data not shown). An embryo treated at HH10 and collected at HH15 shows more post-mitotic cells within the condensing opV nerve/ganglion level caudal to the eye (Figure 3A–B). In an older embryo, treated at HH14 and collected at HH16, still more post-mitotic cells are found within the condensing opV ganglion region (Figure 3C–D). Even later, in an embryo treated at stage HH14, but collected at HH18 when the condensing trigeminal ganglion and opV nerve are easily identifiable (Figure 3E–G), post-mitotic cells are detectable within the opV nerve. The many ^{3}H-Thy labeled nuclei adjacent to and within the opV nerve likely represent dividing neural crest cells. To confirm that these post-mitotic cells within the forming opV nerve are indeed neurons, embryos were stained with the neuronal marker Hu. In an HH17 embryo in a section at forebrain level, just caudal to the eye, Hu+ neurons in the opV nerve can be detected (Figure 3H) in a location rostral to those shown in the latter ^{3}H-Thy treated embryos (Figure 3E–F). The number of Hu+ neurons counted in one ophthalmic nerve at E3 (HH18+) was more than 40 between the opV ganglion and eye level (data not shown). To determine if these cells persist within the ophthalmic nerve, sections were stained with NF to identify the opV nerve and co-stained with Hu to determine if neuronal cell bodies were present within the nerve. At HH24 (E4.5), Hu+ neuronal cell bodies are easily identifiable within the opV nerve (NF+) (Figure 3I–K). Thus, ectodermal trigeminal placodal cells give rise to neurons that persist in the maturing trigeminal ophthalmic nerve.

Cells post-mitotic at HH8 acquire opV placode markers

BrdU labeling allows examination of expression of molecular markers characteristic of the opV placode (Pax3, NF, Hu) in cells that have or will soon exit the cell cycle. As with ^{3}H-Thy, all trigeminal placode cells incorporate BrdU at HH7 (Figure4A) and express Pax3 within the placodal ectoderm by HH9–10 (collected at HH10) (Figure4B,C). Migrating neural crest transiently express Pax3 in the mesenchyme at HH10. Several hours later, a few BrdU- cells were found in the Pax3+ ectoderm and mesenchyme (labeled at HH8, collected at HH13; Figure4D–F). Increasing numbers of Pax3+/BrdU- cells were seen in progressively older embryos when incubated with BrdU (labeled at HH9–10, collected at HH16; Figure4G–L).

The relationship between BrdU uptake and onset of neuronal properties was examined by neurofilament (NFM) expression. As early as HH8 (collected at HH13), a few NFM+/BrdU- cells can be detected (arrow, Figure5A–C, C’’) though the majority of cells are NFM+/BrdU + (arrowhead, Figure 5A–C, C’). Interestingly, some cells have light BrdU labeling, indicating that they are in transition (Figure 5B, C’, arrowhead). Labeling at HH9–10 (collected at HH15) yields a mixture of NFM+/BrdU+ and NFM+/BrdU- (Figure5D–I’’). The results suggest that not all opV placode cells become post-mitotic simultaneously.

While some exit the cell cycle very early and within the placode, others continue to divide for some time.

OpV placode cells are post-mitotic when they initiate expression of neuronal markers

Are cells expressing molecular markers for opV placode cells such as Pax3 and NFM actively cycling, or do they exit the cell cycle and then express these markers? To address this question for the opV placode, either phosphohistoneH3 (PH3) or a short pulse of BrdU were applied to HH9–10 embryos, by which time many opV placode cells are expressing Pax3, to identify actively cycling placodal cells. In contrast to the cumulative labeling experiments, which label all dividing cells during the application, pulse labeling provides a snapshot of time. With a 30 minute application of BrdU, cells undergoing S phase during that time will be labeled. This is balanced with the idea that the cells should not have time to substantially alter protein expression or their physical location.

With rare exceptions, we observed that few Pax3 expressing cells co-express PH3 (data not shown). Because PH3 only marks a subset of the actively dividing cells in mitosis, we also labeled HH9–10 embryos with a short pulse of BrdU (30min.) to identify cells undergoing DNA synthesis and fixed them immediately. Since S phase lasts longer than M, more actively dividing cells are detectable by BrdU than PH3. Interestingly, embryos treated with a short pulse of BrdU yielded both Pax3+/Brdu- and Pax3+/Brdu+ cells (Figure6A–C). The results show that trigeminal placode cells can continue to divide after expressing the specification marker, Pax3 while still in the ectoderm. However, once the placodal Pax3+ cells are in the mesenchyme (starting at HH11), they no longer are dividing (data not shown). The cells that are Pax3 positive within the mesenchyme at HH10 are migrating neural crest cells, which will soon turn off Pax3 expression. The co-labeling of Pax3 with BrdU suggests that some opV placode cells continue to divide at least once even after they initiate expression of the molecular marker Pax3, whereas others are post-mitotic as substantiated by the cumulative labeling experiments (Figure4D–L).

We tested whether dividing opV cells expressed neurofilament (NFM) within the placodal ectoderm and the mesenchyme. We found NFM+ cells are readily identified in the ectoderm and mesenchyme at HH11 (13ss), when opV placode cells first delaminate and enter the mesenchyme (D'Amico-Martel and Noden, 1983; Figure6D–F). When the opV ganglion is well condensed but prior to differentiation of neural crest-derived neurons (HH18), the neuronal marker HuC/D was used to label placodal derived neurons. All HuC/D+ cells are BrdU- indicating that all opV neurons within the condensed ganglion have exited the cell cycle by this stage (Figure6G–I). However, opV placode cells are still being generated within the ectoderm at this stage (data not shown, D'Amico-Martel and Noden, 1980). Our results support the conclusion that some opV cells are post-mitotic very early (HH8) within the placodal ectoderm whereas others continue to be generated throughout gangliogenesis upto HH21 (D'Amico-Martel and Noden, 1980).

Discussion

We find that cells of the presumptive opV placode are actively dividing prior to HH7, but begin exiting the cell cycle as early as HH8 (4ss) and become specified to express Pax3 at HH9–10. However, by the time the first opV placodal neurons delaminate and enter the mesenchyme around HH11, they are no longer dividing. Although specification of the opV placode and expression of Pax3 does not dictate cell cycle exit, it correlates with expression of neuronal markers, NFM and HuC/D, as well as delamination from the ectoderm. Our data suggest that the boundary of the trigeminal placode, previously thought to be the mid-midbrain to rostral hindbrain level, actually includes cells that give rise to neurons within the

opV nerve. As such, ectodermal placode precursors arise in ectoderm as far rostrally as the middle forebrain level.

Early cell cycle exit

We determined the exact timing and nature of the exit of opV placode cells to resolve discrepant information from the literature. Cell cycle exit for opV placode cells previously was proposed to occur from HH13 (Begbie et al., 2002) to as late as HH16 (D'Amico-Martel and Noden, 1980). Many important molecular and cellular events such as specification (Baker et al., 1999) and neurogenesis (Moody et al., 1989; Begbie et al., 2002) are occurring before and during this time period of HH13–16. In order to accurately interpret these processes, it is critical to know when the cells exit the cell cycle.

By using two different methods, ^{3}H-Thy and BrdU labeling, we show that opV placode cells exit the cell cycle starting at HH8 (4ss). At HH6–7, we detect no unlabeled opV placode cells, indicating that these cells are actively dividing. It seems unlikely that the cumulative labeling method fails to detect slowly dividing cells at HH8. First, the cumulative labeling technique for both ^{3}H-Thy and BrdU labeled all cells at HH6–7. Second, post-mitotic cells were first detected at HH8 and continuously increased in numbers at subsequent stages. Third, there was a small time gap (HH8–H10/11) between when cells exit the cell cycle and begin to express neuronal markers such as Brn3a and Neurofilament (Begbie et al., 2002; this paper). Because unlabeled cells (post-mitotic) were detected by HH8 whereas the first placode cells delaminate at HH11 (D'Amico-Martel and Noden, 1983), the results indicate that many opV cells cease dividing well before they begin to ingress from the placodal ectoderm ≥14 hours later at HH11. Additionally, the apparent random distribution of scattered post-mitotic placode cells is similar to dispersion of trigeminal placode cells that has been documented for the trigeminal placode cells at the midbrain and rostral hindbrain levels by transplant studies (D'Amico-Martel and Noden, 1983), mRNA and antibody staining of Pax3 (Stark et al, 1997; Baker et al., 1999), and DiI fate map studies (Xu et al., 2008). Thus, our data suggest that a significant population of opV placode cells are exiting the cell cycle even at HH8.

Cell cycle exit and molecular markers

We correlated the expression of molecular markers with exit of placodal cells from the cell cycle. Previously, Begbie et al. (2002) reported opV placode cells in the mesenchyme at HH13 were not actively cycling as assayed using phosphohistoneH3 and the neuronal marker Islet1. Moody and colleagues (1989) suggested that trigeminal placodal cells did not express the neuronal marker for β-tubulin, TUJ1, until their last cell division. In contrast, some CNS populations can express neuronal markers prior to becoming post-mitotic; e.g. NFM and phosphohistoneH3 are expressed in cycling precursors in the developing retina (McCabe et al., 1999). However, early reticular neurons in the brainstem clearly express NFM after they become post-mitotic (Sechrist and Bronner-Fraser, 1991). Therefore we asked if post-mitotic opV placode cells expressed Pax3 and the neuronal markers of Hu and neurofilament. Interestingly, Pax3, which is expressed in specified opV placode cells (Baker et al., 1999) was found in both actively dividing and quiescent cells. This implies that specification occurs before the final cell division for some opV placode cells. In relation to neurogenesis, only post-mitotic opV placode cells expressed the neuronal markers of Hu and neurofilament. This suggests that although specification occurs around the time of cell cycle exit, the expression of neuronal markers occurs only after the final cell division. Furthermore, all ophthalmic trigeminal placode cells appear to be post-mitotic once they are in the mesenchyme.

We present the previously undocumented finding that opV placode cells express neurofilament while still in the ectoderm at St. 11 (13ss). This implies that the opV placode initiates neurogenesis earlier than other placodes; e.g. the olfactory placode begins neurogenesis at HH13 (Fornaro et al., 2001), epibranchial at HH13–16 (Begbie et al., 1999; Begbie et al., 2002), and otic placode at HH12 (Li et al., 2004).

Rostral extension of opV placode and formation of opV nerve

Surprisingly, we found that some post-mitotic opV placode cells originate further rostrally than indicated by recent fate map studies (Xu et al., 2008). These include cells within the ectoderm adjacent to caudal forebrain and rostral midbrain. Many of these rostral precursors contribute neuronal cell bodies to the opV nerve. Previous work by Covell and Noden (1989) found that some early placode derived neurons are scattered beside the midbrain and above the optic vesicle rather than incorporated into the opV ganglia proper. They hypothesized that these cells eventually shift caudally to become part of the condensing ganglion. However, our data suggest these neurons arise from a rostral extension of the opV placode, adjacent to the forebrain and rostral midbrain.

Interestingly, Hamburger (1961) performed ablation experiments of the placodal ectoderm at variable levels between the eye and otic placode and found this often resulted in ectopic placodal ganglia. Intriguingly, some of these appeared as strings of neurons along the nerves. Hamburger postulated that this could be due to regeneration or incomplete extirpation. Our data support the latter interpretation that these ablations were incomplete, and perhaps when the placodal ectoderm from the caudal forebrain and rostral midbrain are left intact, the rostral part of the opV nerve forms in the absence of the trigeminal ganglion. Similarly, D'Amico-Martel and Noden (1983) used chick-quail transplantation to map the origin of trigeminal neurons. In order to obtain consistent labeling of the trigeminal ganglion, the ectoderm transplant included ectoderm from adjacent to the caudal midbrain. When grafts adjacent to the caudal forebrain and rostral midbrain failed to incorporate label in the trigeminal ganglion, it was assumed that those regions are not part of the ophthalmic trigeminal placode. However, incorporation of these cells into the ophthalmic trigeminal nerve was not examined in detail and may have been missed, later as confirmed by Covell and Noden (1989). Brn3a expression at HH10 also shows individual opV placode cells at rostral as well as caudal midbrain levels (Begbie et al., 2002). Our data support the existence of this apparent post-mitotic population and, additionally, provide evidence that these neurons arise from a rostral extension of the opV placode, adjacent to the caudal forebrain and the rostral midbrain and are maintained in the mature ophthalmic nerve. An intriguing possibility is that these cell bodies within the forming nerve may act as "pioneer" neurons, guiding neurite extension from the ganglion proper.

An additional line of evidence for the rostral extension of the trigeminal placode arose from examination of the trigeminal placode marker Pax3. Although the mRNA for Pax3 in the caudal forebrain and rostral hindbrain was previously published (Stark et al., 1997), until now, this expression has been overlooked. In light of the experiments presented here, it becomes apparent that many of those Pax3+ cells are in fact trigeminal placode cells. It is important to note that although Pax3 is thought of as a marker of specified trigeminal placode cells (Baker et al., 1999), a subpopulation of the cells that initially express Pax3 likely execute the trigeminal placode program. This may explain why the population of trigeminal placode cells exiting the cell cycle appear randomly scattered throughout the ectoderm of the head.

Conclusion

The results reveal several previously unknown properties of the forming opV ganglion and nerve. First, opV placode cells exit the cell cycle early in development, at a time when the majority of embryonic cells are actively dividing. Second, these cells differentiate into neurons shortly thereafter. Third, unlike other peripheral nerves originating from trunk dorsal root ganglia, placode-derived neuronal cell bodies populate the forming opV nerve. The data presented here represent a strong foundation upon which future molecular data regarding trigeminal ganglion formation can be interpreted. Determining the relationship of cell cycle exit to the time of action of growth factors and transcription factors is a critical step for understanding induction and specification of the trigeminal placode cells, whether they end up in the ganglion or nerve.

Supplementary Material

Refer to Web version on PubMed Central for supplementary material.

Acknowledgments

We would like to thank Samuel Ki, Virginia Satterfield, and Dr. Vivian Lee for technical assistance. This work was funded by NIH R01DE16459.

References

Baker CV, Bronner-Fraser M. Vertebrate cranial placodes I. Embryonic induction. Developmental biology. 2001; 232(1):1–61.

Baker CV, Stark MR, Marcelle C, Bronner-Fraser M. Competence, specification and induction of Pax-3 in the trigeminal placode. Development. 1999; 126(1):147–156. [PubMed: 9834194]

Begbie J, Ballivet M, Graham A. Early steps in the production of sensory neurons by the neurogenic placodes. Mol Cell Neurosci. 2002; 21(3):502–511. [PubMed: 12498790]

Begbie J, Brunet JF, Rubenstein JL, Graham A. Induction of the epibranchial placodes. Development. 1999; 126(5):895–902. [PubMed: 9927591]

Covell DA Jr, Noden DM. Embryonic development of the chick primary trigeminal sensory-motor complex. J Comp Neurol. 1989; 286(4):488–503. [PubMed: 2778103]

D'Amico-Martel A, Noden DM. An autoradiographic analysis of the development of the chick trigeminal ganglion. J Embryol Exp Morphol. 1980; 55:167–182. [PubMed: 6966308]

D'Amico-Martel A, Noden DM. Contributions of placodal and neural crest cells to avian cranial peripheral ganglia. Am J Anat. 1983; 166(4):445–468. [PubMed: 6858941]

Fornaro M, Geuna S, Fasolo A, Giacobini-Robecchi MG. Evidence of very early neuronal migration from the olfactory placode of the chick embryo. Neuroscience. 2001; 107(2):191–197. [PubMed: 11731093]

Gratzner HG. Monoclonal antibody to 5-bromo- and 5-iododeoxyuridine: A new reagent for detection of DNA replication. Science. 1982; 218(4571):474–475. [PubMed: 7123245]

Hamburger V. Experimental analysis of the dual origin of the trigeminal ganglion in the chick embryo. J Exp Zool. 1961; 148:91–117. [PubMed: 13904079]

Hamburger V, Hamilton HL. A series of normal stage in the development of the chick embryo. Journal of Morphology. 1951; 88(1):49–91.

Harris J, Ayyub C, Shaw G. A molecular dissection of the carboxyterminal tails of the major neurofilament subunits NF-M and NF-H. J Neurosci Res. 1991; 30(1):47–62. [PubMed: 1724473]

Hendzel MJ, Wei Y, Mancini MA, Van Hooser A, Ranalli T, Brinkley BR, Bazett-Jones DP, Allis CD. Mitosis-specific phosphorylation of histone H3 initiates primarily within pericentromeric heterochromatin during G2 and spreads in an ordered fashion coincident with mitotic chromosome condensation. Chromosoma. 1997; 106(6):348–360. [PubMed: 9362543]

Langman J, Guerrant RL, Freeman BG. Behavior of neuro-epithelial cells during closure of the neural tube. J Comp Neurol. 1966; 127(3):399–411. [PubMed: 5968003]

Lee VM, Sechrist JW, Luetolf S, Bronner-Fraser M. Both neural crest and placode contribute to the ciliary ganglion and oculomotor nerve. Developmental biology. 2003; 263(2):176–190. [PubMed: 14597194]

Li H, Liu H, Sage C, Huang M, Chen ZY, Heller S. Islet-1 expression in the developing chicken inner ear. J Comp Neurol. 2004; 477(1):1–10. [PubMed: 15281076]

Marusich MF. Differentiation of neurogenic precursors within the neural crest cell lineage. Brain Res Bull. 1993; 30(3–4):257–263. [PubMed: 8457874]

McCabe KL, Bronner-Fraser M. Essential role for PDGF signaling in ophthalmic trigeminal placode induction. Development. 2008; 135(10):1863–1874. [PubMed: 18417621]

McCabe KL, Gunther EC, Reh TA. The development of the pattern of retinal ganglion cells in the chick retina: mechanisms that control differentiation. Development. 1999; 126(24):5713–5724. [PubMed: 10572047]

McCabe KL, Manzo A, Gammill LS, Bronner-Fraser M. Discovery of genes implicated in placode formation. Developmental biology. 2004; 274(2):462–477. [PubMed: 15385172]

McCabe KL, McGuire C, Reh TA. Pea3 expression is regulated by FGF signaling in developing retina. Dev Dyn. 2006; 235(2):327–335. [PubMed: 16273524]

McCabe KL, Shiau CE, Bronner-Fraser M. Identification of candidate secreted factors involved in trigeminal placode induction. Dev Dyn. 2007; 236(10):2925–2935. [PubMed: 17879314]

Meyer JS, Nauert J, Koehm S, Hughes J. Cell kinetics of human tumors by in vitro bromodeoxyuridine labeling. J Histochem Cytochem. 1989; 37(9):1449–1454. [PubMed: 2768814]

Moody SA, Quigg MS, Frankfurter A. Development of the peripheral trigeminal system in the chick revealed by an isotype-specific anti-beta-tubulin monoclonal antibody. J Comp Neurol. 1989; 279(4):567–580. [PubMed: 2918088]

Sechrist J, Bronner-Fraser M. Birth and differentiation of reticular neurons in the chick hindbrain: ontogeny of the first neuronal population. Neuron. 1991; 7(6):947–963. [PubMed: 1764246]

Sechrist J, Marcelle C. Cell division and differentiation in avian embryos: techniques for study of early neurogenesis and myogenesis. Methods Cell Biol. 1996; 51:301–329. [PubMed: 8722483]

Sechrist J, Nieto MA, Zamanian RT, Bronner-Fraser M. Regulative response of the cranial neural tube after neural fold ablation: spatiotemporal nature of neural crest regeneration and up-regulation of Slug. Development. 1995; 121(12):4103–4115. [PubMed: 8575311]

Sidman, RL. Autoradiographic methods and principles for study of the nervous with thymidine-H3. In: Nauta WJHaE, SOE., editor. New York: Springer-Verlag; 1970.

Stark MR, Sechrist J, Bronner-Fraser M, Marcelle C. Neural tube-ectoderm interactions are required for trigeminal placode formation. Development. 1997; 124(21):4287–4295. [PubMed: 9334277]

Venters SJ, Argent RE, Deegan FM, Perez-Baron G, Wong TS, Tidyman WE, Denetclaw WF Jr, Marcelle C, Bronner-Fraser M, Ordahl CP. Precocious terminal differentiation of premigratory limb muscle precursor cells requires positive signalling. Dev Dyn. 2004; 229(3):591–599. [PubMed: 14991714]

Xu H, Dude CM BakerCV. Fine-grained fate maps for the ophthalmic and maxillomandibular trigeminal placodes in the chick embryo. Developmental biology. 2008; 317(1):174–186. [PubMed: 18367162]

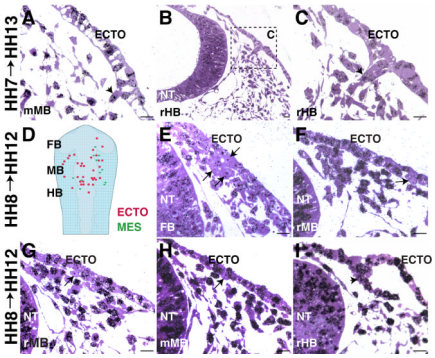

Figure 1.

Some opV placode cells are post-mitotic by HH8 (3–5ss). A–C. All cells are labeled in embryos treated with ^{3}H-Thy at HH7 (1ss) (collected at HH13 (18ss)). A. High power of opV placode cell (arrowhead) delaminating at mid-midbrain (mMB) level. B–C. At rostral hindbrain levels (rHB), spurs of cells delaminating from ectoderm were actively dividing at HH7 (arrowhead). D. Diagram of HH12 (15ss) embryo showing relative location of HH8 (4ss) post-mitotic cells in ectoderm (red circles) and mesenchyme (green triangles). E–I. Embryos treated with ^{3}H-Thy at HH8 (4ss) (collected at HH12 (15ss)). E. Cluster of cells (arrows) have exited cell cycle by HH8 (4ss) at caudal forebrain level. F–G. Individual cells at rostral midbrain level have exited cell cycle and are delaminating. H. At mMB, a cell in ectoderm has exited the cell cycle (arrow). I. At rHB, most cells are labeled; a spur of opV cells actively dividing at HH8 (arrowhead). A–C, E–I. Large arrows indicate post-mitotic cells and arrowheads indicate cells in S phase at time of initial ^{3}H-Thy. ECTO=ectoderm, NT=neural tube. Scale bars are approximately 10 μm.

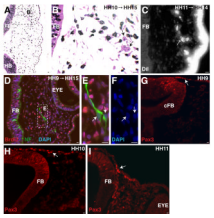

Figure 2.

Trigeminal placode extends into caudal forebrain level. A. At the forebrain/eye level, an HH10 (9ss) embryo (collected at HH15 (25ss)) shows two post-mitotic cells (arrows) that migrated to position of future opV nerve. B. Higher power of A. C. DiI label at HH11 (12ss) (collected at HH14 (21ss)) shows delaminate placode cells at forebrain level (small arrow). D. Embryo treated at HH9 (8ss) (collected at HH15 (26ss)) (same level as A,B) has two NFM+/BrdU- cells. E. Higher power of D. F. DAPI of cells in E. G–I. Pax3, a marker for specified trigeminal placode cells, is expressed at forebrain levels at HH9, 10, 11 (8ss, 11ss, 14ss). A–F. Large arrows indicate post-mitotic cells. G–I. Large arrow indicates Pax3+ cell in ectoderm. FB=forebrain, cFB=caudal forebrain, HB=hindbrain. Scale bars are approximately 10 μm. Magenta/green version (without DAPI triple label) can be found in Supplemental Figure1.

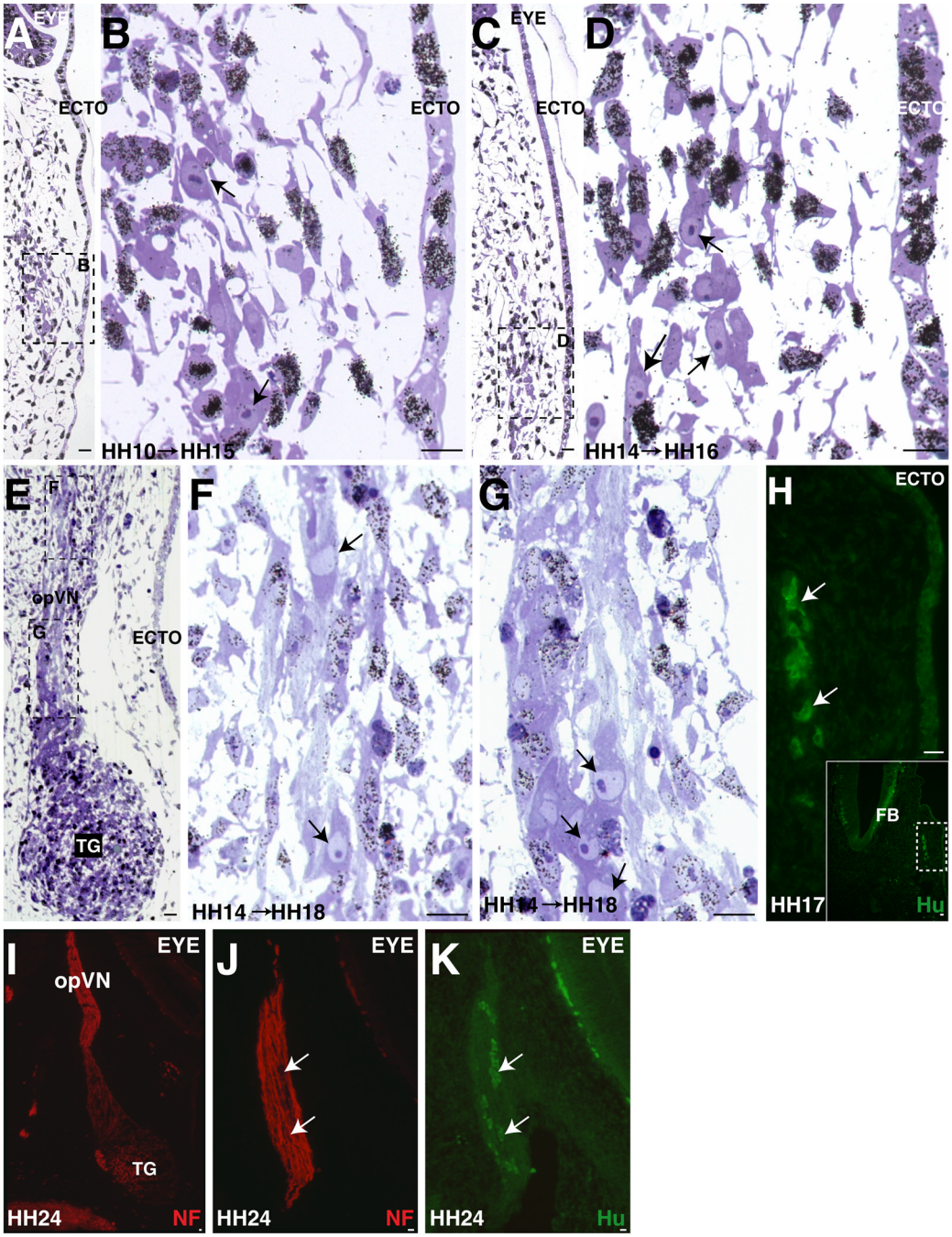

Figure 3.

Post-mitotic opV placode cells increase in number over time and become localized in condensing opV ganglion and nerve. A–B. Between mid-eye level and opV ganglion region, the number of post-mitotic cells within the forming opV nerve (B) by this stage are increasing to 2–5 per section in an embryo treated at HH10 (9ss) and collected at HH15 (25ss). C–D. At a similar axial level in an older embryo treated at HH14 (22ss) and collected at HH16 (28ss), additional post-mitotic cells can be found within the condensing opV nerve approaching the ganglion region. E–G. As a comparison to C-D, this embryo was treated at the same time as C–D at HH14 (23ss) but allowed to develop until HH18 (36ss). In a longitudinal section at the level of the condensed trigeminal ganglion (contains opV and

mmV cells at this level), post-mitotic cells are seen in the opV nerve (E) both rostral towards the eye (F) and caudal at the ganglion edge (G). H. Hu+ neurons (white arrows) are shown in the forming opV at the level of forebrain caudal to the eye at HH17 (29ss). I. Expression of NF at level of opV nerve at HH24. J. Adjacent section of I shows NF expression within opV nerve. K. Nerve cell bodies are Hu+ within the maturing opV nerve. A–G. Black arrows indicate post-mitotic cells. ECTO= ectoderm, TG= trigeminal ganglion, FB= forebrain, opVN= ophthalmic trigeminal nerve. Scale bars are approximately 10 μm. Magenta/green version can be found in Supplemental Figure2.

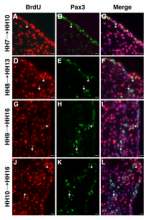

Figure 4.

opV placode cells that express Pax3 begin exiting cell cycle at HH8 (3–5ss). A–C. All ectoderm cells that give rise to future Pax3+ opV placode cells are actively dividing at HH7 (2ss) (collected at HH10 (11ss)). Pax3 stains migrating neural crest in the mesenchyme at HH10. D–F. Pax3+/BrdU- cells detected in the mesenchyme first treated at HH8 (5ss) (collected at HH13 (19ss)) similar to embryo treated with ^{3}H-Thy. G–I. More Pax3+/BrdU- cells become detectable in a spur of delaminating cells when treated at HH9 (8ss) (collected at HH16 (28ss)). J–L. Additional placode cells exiting the cell cycle by HH10 (11ss) (collected at HH16 (28ss)). All sections at level of middle midbrain. BrdU (red;A,D,G,J); Pax3 (green;B,E,H,K); Merge of BrdU, Pax3, DAPI (blue;C,F,I,L). Arrows indicate post-mitotic cells and arrowheads indicate cells undergoing DNA synthesis at time of initial BrdU application. Scale bars are approximately 10 μm. Magenta/green version (without DAPI triple label) can be found in Supplemental Figure3.

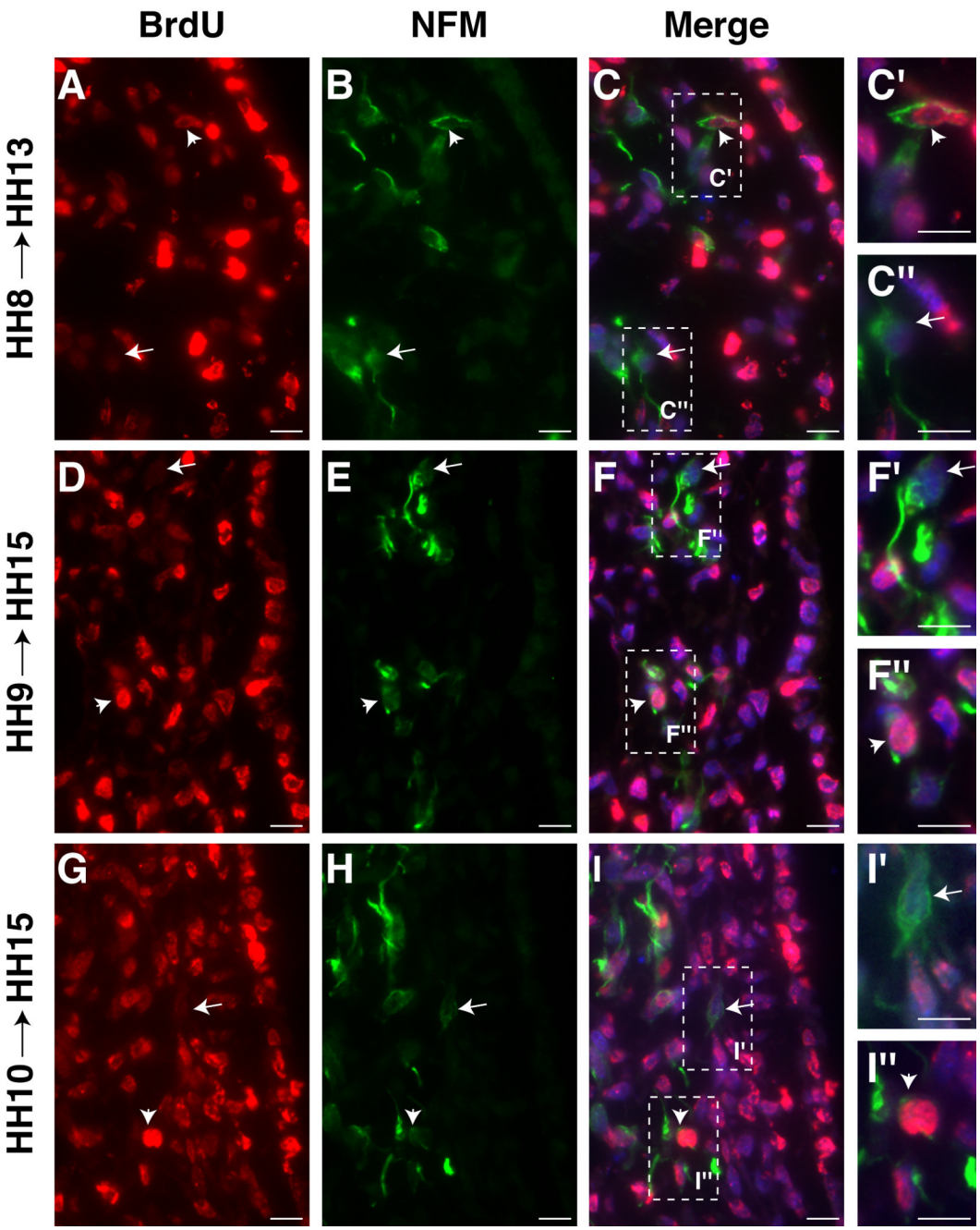

Figure 5.

opV placode cells that express NFM, begin exiting cell cycle at HH8 (3–5ss). A–C. A few NFM+/BrdU- cells detected in embryos treated at HH8 (5ss) (collected at HH13 (18ss)). C'. Higher power view of C showing NFM+/BrdU+ cell. C''. Higher power view of C showing NFM+/BrdU- cell. D–F. More NFM+/BrdU- cells in embryos treated at HH9 (8ss) (collected at HH15 (26ss)). F'. Higher power view of F showing NFM+/BrdU- cell. F''. Higher power view of F showing NFM+/BrdU+ cell. G–I. Additional placode cells have exited the cell cycle by HH10 (9ss) and express NFM (collected at HH15 (25ss)). I'. Higher power view of I showing NFM+/BrdU- cell. I''. Higher power view of I showing NFM+/BrdU+ cell. Arrows indicate post-mitotic cells and arrowheads indicate cells undergoing

DNA synthesis at time of initial BrdU application. BrdU (red;A,D,G); NFM (green;B,E,H); Merge of BrdU, NFM, DAPI (blue;C,F,I). All sections at level of middle midbrain. Scale bars are approximately 10 μm. Magenta/green version (without DAPI triple label) can be found in Supplemental Figure4.

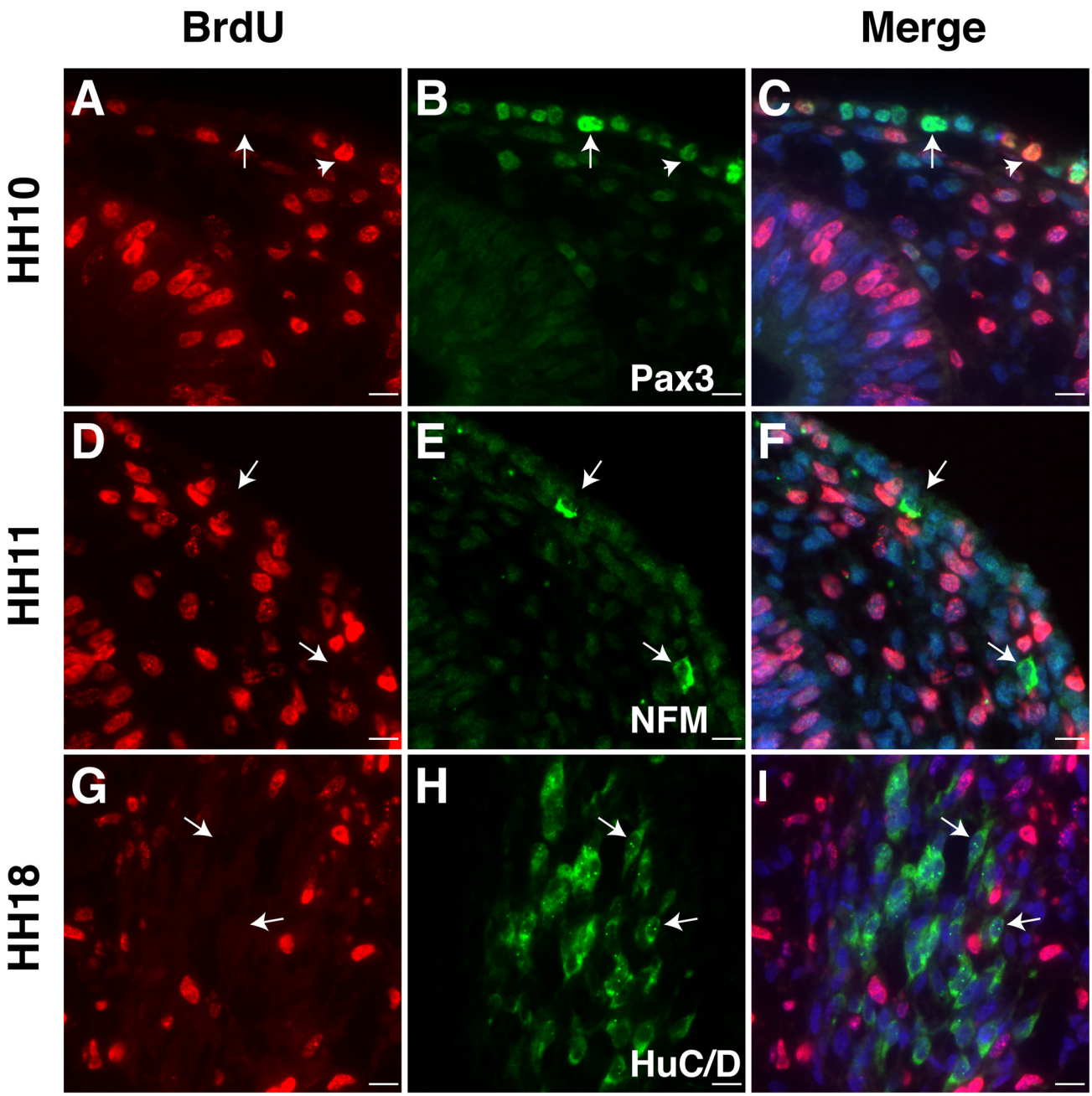

Figure 6.

Pulse of BrdU shows opV placode cells that express neuronal markers have exited the cell cycle. Embryos were exposed to a 30 minute pulse of BrdU immediately before fixation. A–C. However, Pax3 expression does not necessarily correlate with cell cycle exit. At HH10 (10ss), opV placode cells in ectoderm express Pax3 (green) with (arrowhead) and without (arrow) BrdU. D–F. At HH11 (13ss), NFM+ (green)/BrdU- cells are detected in ectoderm and mesenchyme. G–I. By HH18 (33ss), opV placode cells condensing in opV ganglion are Hu+ (green)/Brdu-(arrows). A–F at level of mid midbrain, G–I at level of caudal midbrain. Scale bars are approximately 10 μm. Magenta/green version (without DAPI triple label) can be found in Supplemental Figure5.